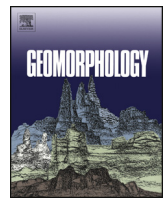




Contents lists available at ScienceDirect

Geomorphology

journal homepage: www.elsevier.com/locate/geomorph

Remote sensing as tool for development of landslide databases: The case of the Messina Province (Italy) geodatabase

Andrea Ciampalini ^{a,*}, Federico Raspini ^a, Silvia Bianchini ^a, William Frodella ^a, Federica Bardi ^a, Daniela Lagomarsino ^a, Federico Di Traglia ^a, Sandro Moretti ^a, Chiara Proietti ^b, Paola Pagliara ^b, Roberta Onori ^b, Angelo Corazza ^b, Andrea Duro ^b, Giuseppe Basile ^c, Nicola Casaglia ^a

^a Department of Earth Science, University of Firenze, via La Pira 4, Firenze 50121, Italy

^b Italian Civil Protection Department (DPC), via Vitorchiano 2, Roma 00189, Italy

^c Regional Department of Civil Protection (DRPC), Hydrogeological and Environmental Risks Service and Service for Messina Province, Italy

ARTICLE INFO

Article history:

Received 27 August 2014

Received in revised form 21 January 2015

Accepted 23 January 2015

Available online xxx

Keywords:

Geodatabase

Landslide

Remote sensing

Risk

Civil Protection

Hazard

ABSTRACT

Landslide geodatabases, including inventories and thematic data, today are fundamental tools for national and/or local authorities in susceptibility, hazard and risk management. A well organized landslide geo-database contains different kinds of data such as past information (landslide inventory maps), ancillary data and updated remote sensing (space-borne and ground based) data, which can be integrated in order to produce landslide susceptibility maps, updated landslide inventory maps and hazard and risk assessment maps. Italy is strongly affected by landslide phenomena which cause victims and significant economic damage to buildings and infrastructure, loss of productive soils and pasture lands. In particular, the Messina Province (southern Italy) represents an area where landslides are recurrent and characterized by high magnitude, due to several predisposing factors (e.g. morphology, land use, lithologies) and different triggering mechanisms (meteorological conditions, seismicity, active tectonics and volcanic activity). For this area, a geodatabase was created by using different monitoring techniques, including remote sensing (e.g. SAR satellite ERS1/2, ENVISAT, RADARSAT-1, TerraSAR-X, COSMO-SkyMed) data, and in situ measurements (e.g. GBInSAR, damage assessment). In this paper a complete landslide geodatabase of the Messina Province, designed following the requirements of the local and national Civil Protection authorities, is presented. This geo-database was used to produce maps (e.g. susceptibility, ground deformation velocities, damage assessment, risk zonation) which today are constantly used by the Civil Protection authorities to manage the landslide hazard of the Messina Province.

© 2015 The Authors. Published by Elsevier B.V. This is an open access article under the CC BY-NC-ND license (<http://creativecommons.org/licenses/by-nc-nd/4.0/>).

1. Introduction

Geodatabases dedicated to landslides, including inventories and thematic data, represent a powerful tool for users operating at different administrative and organizational levels, from local to continental (Guzzetti et al., 1994; Dellow et al., 2003; Gaspar et al., 2004; Colombo et al., 2005; Devoli et al., 2007; Gustavsson et al., 2008; Suprechi et al., 2010; Van den Eeckhaut and Hervás, 2012; Battistini et al., 2013; Klose et al., 2014; Pereira et al., 2014; Zêzere et al., 2014). The potential of a geodatabase is given by past information (landslide inventory maps, LIM) combined with geoenvironmental and triggering factors, in order to produce useful maps (e.g. landslide susceptibility map, LSM, map of the element at risk) and to manage the different emergency cycle phases (van Westen et al., 2005). Furthermore all of these data and products, organized into a GIS database, can be easily updated when

new acquired data are included. GIS technologies facilitate the management of different typology of analogical data, maintaining a proper cartographic representation (Guzzetti et al., 2012) and allowing the combination of analogue and vector data in order to create useful hazard management maps. These different information, included in the GIS geodatabase maintain their geometric consistency, allowing rapid query and calculation using the stored data (e.g. landslide area, typology, hazard degree).

In Italy, landslides are recurrent phenomena causing victims and significant economic damage to buildings and infrastructures, loss of productive soils and pasture lands. Annually, during the rainy seasons (from September to November and from March to June) the Italian regions are affected by natural hazards, among which landslides represent the primary cause of death (Guzzetti, 2000).

The Sicily Region (southern Italy) and in particular the Messina Province is an area prone to landslide hazard due to several predisposing factors (morphology, land use, lithologies) and of different triggering mechanisms as meteorological conditions (Del Ventisette et al., 2012),

* Corresponding author. Tel.: +39 0552757548; fax: +39 0552756323.
E-mail address: andrea.ciampalini@unifi.it (A. Ciampalini).

seismicity, active tectonics (Billi et al., 2008) and volcanic activity (Intrieri et al., 2013; Nolesini et al., 2013). For instance, between 2009 and 2010 in both the Messina Province mountain ranges (Nebrodi and Peloritani), several municipalities were affected by more than a thousand different types of mass movements (i.e. debris flows, complex, rotational and translational landslides, rock falls). These landslides caused more than 37 victims and severe damage to urbanized areas, infrastructures (national highways, rural roads and railroads), cultivated and pasture lands. The blocking of rural roads left several towns isolated causing serious difficulties in the rescue activities. Some of these events occurred in areas characterized by low to null landslide hazard, affecting urbanized areas considered as safe, suggesting that the previously available landslide information and mapping underestimated the potential hazard of this area. From the beginning of this emergency phase the Civil Protection System was promptly activated, in order to manage the landslide risk, involving the Civil Protection Departments at both National (DPCN) and Regional (DPRC) levels, the Environmental Department and other local authorities and research centers (Pagliara et al., 2014).

In the framework of the post-disaster phase led by the DPCN, several activities were performed aimed at supporting local authorities in the hydrogeological risk assessment and management. Following the above mentioned events the Messina Province drew the attention of many geoscientists, becoming test site of the FP7 European projects DORIS (www.doris-project.eu) and LAMPRE (www.lampre-project.eu). Within these projects all the previously available data (thematic maps, Digital Elevation Model, VHR optical photos) and newly acquired data (optical and Synthetic Aperture Radar, SAR), were integrated into an homogenized GIS geodatabase. All these data were used in order to improve the products (e.g. landslide inventory maps, ground deformation velocity maps, residual risk zonation), and their value added in landslide mapping, monitoring and forecasting activities.

In the Messina Province, a geodatabase was used to include different products created by means of advanced monitoring techniques, comprising remote sensing (optical and SAR) and in situ (Ground Based-Interferometric SAR, GBInSAR) data. In particular, remotely sensed data acquired through different SAR satellites (ERS1/2, ENVISAT, RADARSAT-1, TerraSAR-X, COSMO-SkyMed) were used in order to monitor the long term slope deformation evolution. The long time displacement series obtained by combining ERS1/2 and ENVISAT data (1992–2010) and different sensors (C- and X- band) allowed to update the landslide state of activity and to refine the extension of single landslides by comparing the ground deformation velocities measured in different periods.

In this paper the structures and contents of the Messina Province landslide geodatabase are described. Furthermore, some very useful products at different scales generated by the combination of LIMS, thematic data and remote sensing methodologies are presented, highlighting their use by the Civil Protection authorities.

2. Study area

The study area (Messina Province) is located in southern Italy, in Sicily's North-Eastern sector (Fig. 1). From a geologic point of view the Messina Province is part of the Sicilian fold-and-thrust orogenic belt formed during the Tertiary due to the convergence between the European and African plates (Dewey et al., 1989; De Guidi et al., 2013). This belt is made of three different tectono-stratigraphic zones overthrust on a buried structural domain (Di Paolo et al., 2014). The internal orogenic sector corresponds to the Peloritani Mountains which are made of crystalline rocks and a Meso-Cenozoic sedimentary cover (Messina et al., 2004). The Central Zone (Sicilidi Units) represents the accretionary wedge (upper Cretaceous–lower Miocene pelagic succession) formed by the remnants of the Neotethyan wedge (Corrado et al., 2009). The External Zone (upper Oligocene–middle Miocene clastic sediments) is represented by the Numidian Flysch Units (Carbone et al., 1990; Thomas et al., 2010). Rocks belonging to

the Central and External Zones crop out within the Nebrodi Mountains. From North-East to South-West several wedge-top deposits (Oligocene–Pliocene) can be recognized (Di Paolo et al., 2014). Along the Tyrrhenian and Ionian coasts several normal faults formed small extensional basins during the Pleistocene, filled by terrigenous deposits (Di Stefano et al., 2012).

The geostructural conditions, the competence of the outcropping rocks and the tectonic activity strongly influence the morphology of the area. The coastal landscape is typical for recently uplifted areas: steep slopes, narrow valleys and high relief energy are the main geomorphologic features. The morphometric characteristics of the river basins are represented by straight and parallel hydrographic networks influenced by the short distance separating the watershed from the coast. River catchments have a narrow width with significant transport of solid materials; incisions are short and deeply entrenched into V-shaped valleys, especially in the mountainous sectors. Several small alluvial plains, formed where riverbeds become over-flooded, characterize the coastal area.

Forming a hydrographic point of view, the presence of straight, steep course, gravel-bed river draining mountain areas is the most evident feature. Their presence is typical for the Mediterranean climate region and their flow varies seasonally and their regime is torrential with catastrophic transport of solid materials following heavy rainfall, causing severe damage if flooding occurs close to densely populated centers.

Intense and exceptional rainfall events were the main triggering factors which, combined with predisposing factors such as weak lithologies and the steep slopes, caused several mass movements in the Messina Province, such as: debris flow, rotational and translational slides, rock falls and shallow and deep-seated landslides.

2.1. The event of autumn 2009

On October 1st 2009, a high intensity storm hit the Ionian side of Sicily, particularly affecting a restricted area in the south-western part of Messina Province, between the Peloritani Mountains ridge and the coastline (Fig. 1) (Ardizzone et al., 2012; Del Ventisette et al., 2012). In this zone, the main built-up areas are concentrated along the coastline. The hilly area is characterized by the presence of smaller settlements (e.g. Briga, Giampileri, Altolia) which are connected with the urbanized coastal area by a single provincial road climbing upward along very steep slopes.

The St. Stefano di Briga rain gauge (Fig. 1) recorded a rainfall of 225 mm in 8 h, with a peak of 115 mm in 3 h. The heavy precipitation of October 1st further reduced the slope stability conditions, already undermined by the significant accumulation of rainfall that had occurred during the month of September, which led to complete soil saturation. During the same day, the persistent rainfall triggered more than 600 slope failures, mainly shallow soil slides, debris avalanches, and debris and mud flows over an area of about 50 km². The more severe damage was reported in the villages of Giampileri, Scaletta Zanclea, Guidomandri, Pèzzolo, Altolia, and Itàla. Landslides damaged many roads as well as the railway system and main highways. The assessed number of fatalities caused by landslides and inundation amounted to 37 (including 31 deaths and 6 missing persons), with 122 injured people and 2019 evacuated people.

2.2. The event of winter 2010

Between 2009 and 2010 several municipalities (San Fratello, Caronia, Naso, Ucria, and many others) located in the Nebrodi Mountains, a 70 km long ENE-WSW trending mountain chain, spanning in altitude from the sea level to 1847 m (Fig. 1), were intensely affected by several slope instability phenomena that caused intense damages to buildings and infrastructures (Del Ventisette et al., 2013; Bardi et al., 2014; Bianchini et al., 2014a,b; Ciampalini et al., 2014). This area located in the western part of the Messina Province was affected mainly by

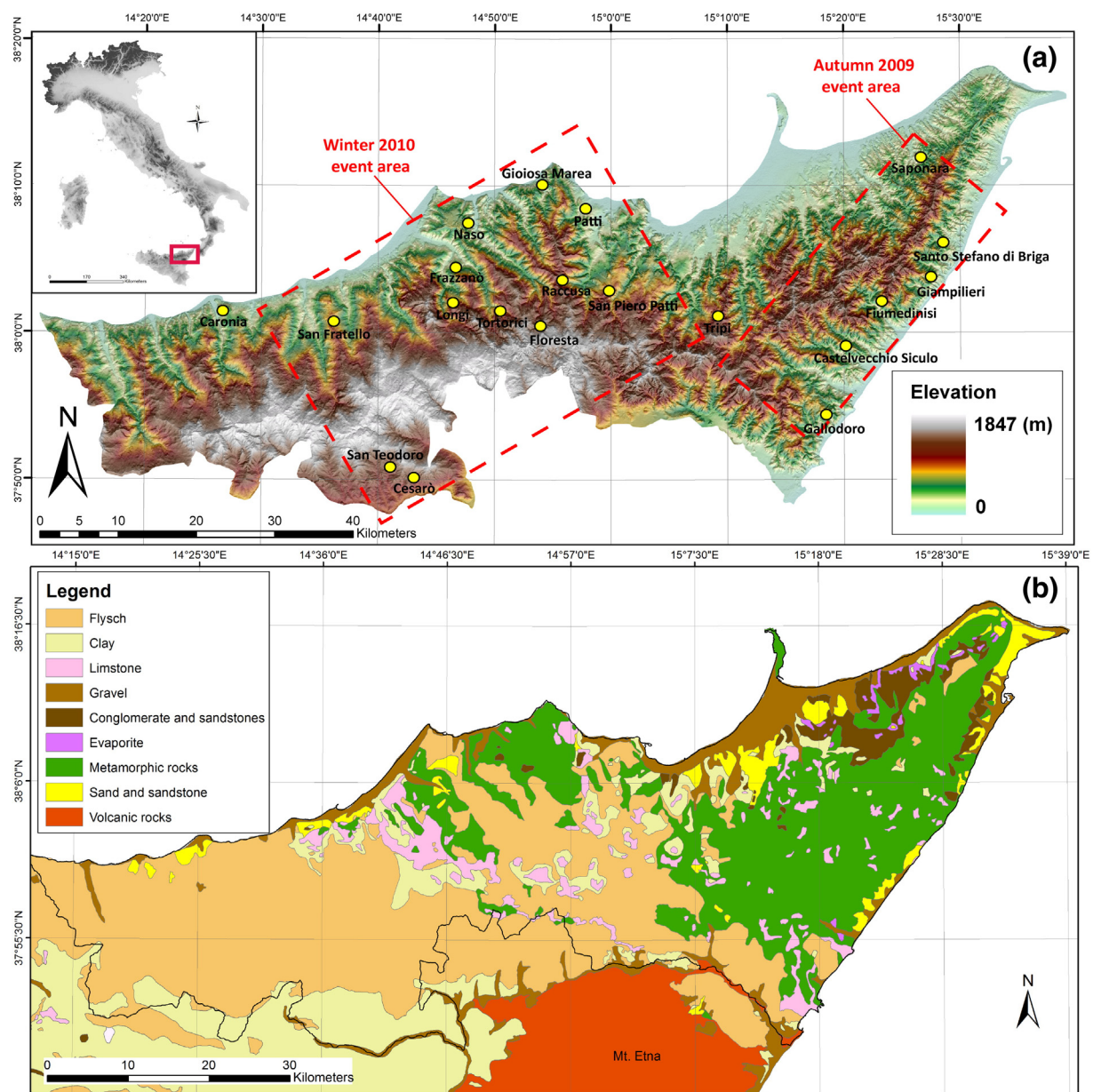


Fig. 1. (a) Location of the study area. Dots represent the municipalities affected by landslide phenomena between 2009 and 2010. (b) Geolithological map of the Messina Province. (See online version for color images).

complex, rotational and deep-seated phenomena. The deformation velocity, slower with respect to those of the debris flows that occurred in the Peloritani Mountains autumn 2009 event, prevented the presence of victims but the damage to buildings and infrastructures was severe.

Following this event, in the framework of the post-disaster initiatives lead by the National Department of Civil Protection, several activities were performed aimed at supporting local authorities in the hydrogeological risk assessment. In particular, a detailed geomorphologic analysis, exploiting the contribution of PSInSAR™ technique and photo interpretation, was performed by the Earth Science Department of the University of Florence (DST-UNIFI, Centre of Competence of the Italian Civil Protection for geo-hazards) in order to identify slow moving pre-existing landslides affecting the whole territory hit by a heavy rainfall period.

3. Methods

The database of the Messina Province was developed in three different phases: (i) data collection; (ii) database design; and (iii) product

generation. The collected data can be divided into two categories: (i) ancillary data and (ii) space-borne SAR data (Fig. 2).

3.1. Data collection

3.1.1. Ancillary data

Ancillary data included in the database are represented by different thematic maps (geological, topographical, building and infrastructure maps, land cover, and pre-existing landslide inventory maps, Digital Elevation Model, VHR optical photos). The geology of the study area was retrieved using the geological map of the Messina Province (scale 1:50,000) in digital format. The land cover was deduced by the updated (2000) Corine Land Cover map (scale 1:100,000). Each polygon was classified following the three levels of the Corine Land Cover classification (<http://www.eea.europa.eu/publications/COR0-landcover>). The C.T.R. (Carta Tecnica Regionale, scale 1:10,000) in vector format was used for the topography and for the localization of buildings and infrastructures. Slope and aspect maps of the Messina Province were produced using a DEM with a 20 × 20 m resolution generated by the

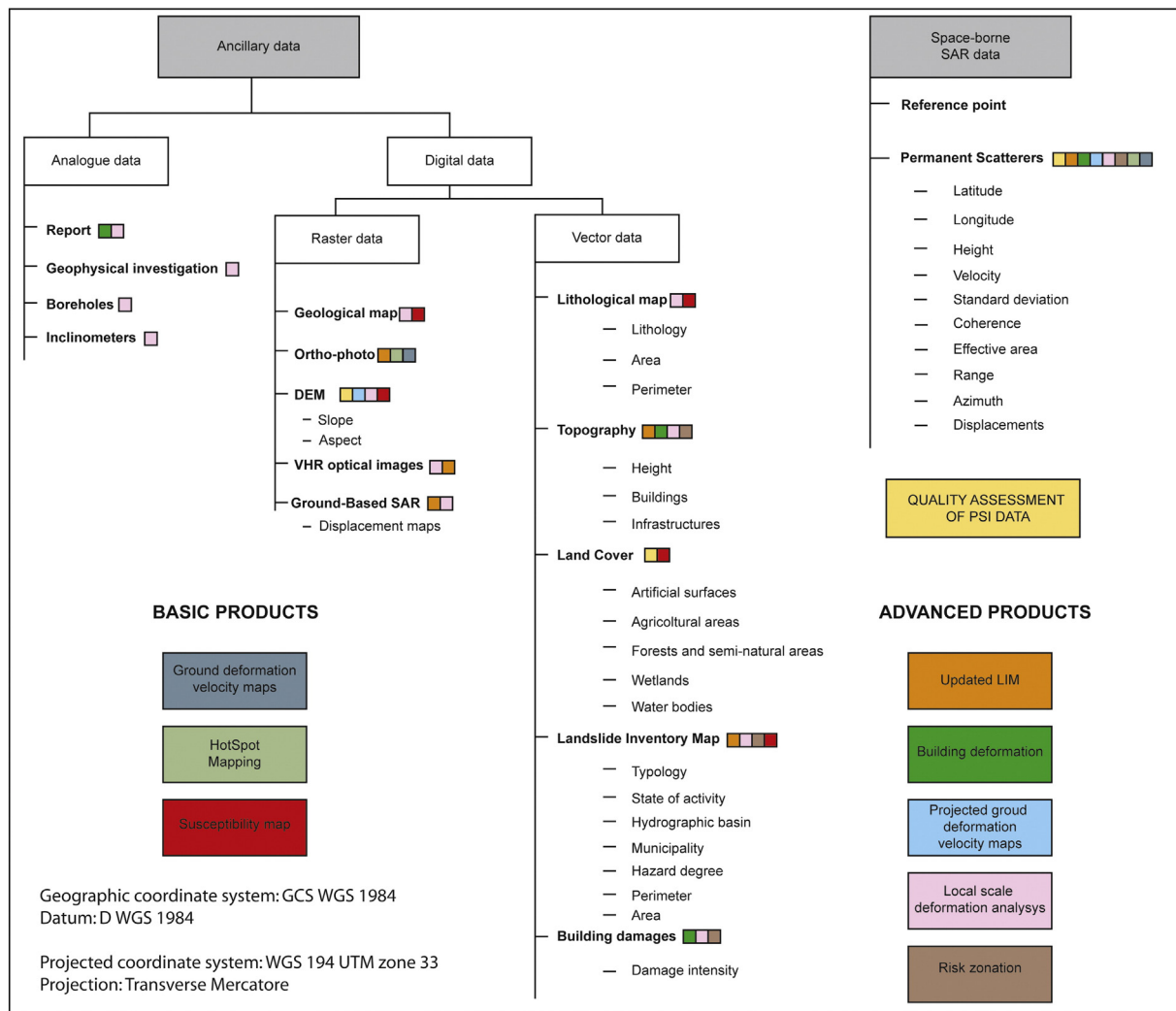


Fig. 2. Flow chart showing the design of the Messina Province geodatabase and how the single layers were used and combined in product generation. Data were divided between available ancillary data and new acquired space-borne SAR data. (See online version for color image).

Istituto Geografico Militare (IGM). An orthophoto (Volo Italia 2000, 1 m of pixel resolution) of the Sicily Region was used as reference map. Quickbird VHR-optical images were also used for specific areas. Usually, these images were acquired before and after major investigated events such as those occurred in Giamplieri and in San Fratello between October 2009 and February 2010.

The landslide inventory map of the Sicily Region (PAI – Piano di Assetto Idrogeologico) was produced between 2005 and 2007 and contains information about 32,669 slope instability phenomena distributed within the Sicily Region. Among the mapped landslides, 9358 phenomena (28.65%) are located within the Messina Province. A smaller part of the inventory (about the 5%) is updated up to 2012. Each landslide is represented by a polygon which is linked to an attribute table where the related available data (ID, hydrographic basin, province, municipality, typology, state of activity, hazard degree, perimeter, area) are reported.

The database includes very detailed information regarding specific municipalities damaged by severe events during the last five years. For example internal reports of the Regional Civil Protection Department are available for several municipalities (e.g. Caronia, San Fratello, Naso, Castell'Umberto). These reports contain detailed information related to single landslides (inclinometers, geophysical investigations, boreholes, fracture patterns, building and infrastructure damage assessment maps).

In particular for the San Fratello Municipality ground displacement maps are also available. They were obtained using a ground based radar which started to acquire data since March 10th 2010.

3.1.2. Space-borne SAR data

Ground displacement measurements were obtained for the Nebrodi and Peloritani mountain ranges using the SqueeSAR™ technique (Ferretti et al., 2011). Developed by T.R.E. (Tele-Rilevamento Europa, a spin-off company of the Polytechnic University of Milano), the SqueeSAR approach is a second generation PSInSAR algorithm (Ferretti et al., 2000, 2001), one of many different approaches (Raucoles et al., 2009) based on the processing of several (at least 15), co-registered, multi-temporal satellite SAR images of the same target area. The main idea behind the PSInSAR method is to analyze the backscattered signal from the observed scene to identify ground elements (temporally stable from an electromagnetic point of view) characterized by high reflectivity (Persistent Scatterers, PSs) (Ferretti et al., 2000, 2001; Werner et al., 2003). A single PS exhibits reduced temporal decorrelation due to its high electromagnetic reflectivity and its coherent, point-like, stable scattering behavior. Having a stable radar signature, PSs are only slightly affected by decorrelation phenomena and the level of backscattered signal is much higher than the inherent noise of the sensor (i.e., the signal-to-noise ratio is extremely high).

The development of the SqueeSAR method (Ferretti et al., 2011) allows a step ahead in the conventional processing techniques and has proven to successfully overcome the main limitations of the pixel-based analysis. In fact, in natural, less urbanized and agricultural environments, PSInSAR technique partially fails due to complete decorrelation of a great number of scatterers. SqueeSAR technique provides a significantly increased coverage of ground deformation measurement points, especially over non-urban areas (Meisina et al., 2013; Bellotti et al., 2014), detecting not only point-wise Permanent Scatterers (as the PSInSAR technique) but also spatially Distributed Scatterers (DSs). This challenging new approach is capable of obtaining reliable ground displacement measurement, retrieving electromagnetic information not only from point-wise, corner reflector-like objects (i.e., PS), but also from DSs, identified in low-reflectivity homogeneous areas, such as scattered outcropping rocks, debris flows, non-cultivated lands and arid areas.

A number of satellite SAR datasets were acquired and processed to produce ground deformation maps for the investigated areas. SAR images acquired by C-band (ERS 1/2, ENVISAT and RADARSAT-1) and by X-band (COSMO-SkyMed, CSK and TerraSAR-X) were collected and processed (Table 1). Processed SAR data include both pre-event images (for the mapping of pre-existing extremely slow to very slow moving landslides) and post-event information (exploited to assess residual movements and deformation).

An attribute table is associated to each interferometric dataset, including: (i) PS identifier (ID); (ii) geographic coordinates (Latitude, Longitude); (iii) height; (iv) average velocity and the related standard deviation; (v) coherence degree and (vi) the cumulative displacement for each acquisition date, expressed in millimeters. The latter fields are used to retrieve time displacement series.

3.2. Database design

The database was created between 2010 and 2013, within the European Union's Seventh Framework Programme for Research Project "Advanced downstream service for the detection, mapping, monitoring and forecasting of ground deformations" (FP7 DORIS Project). The aim was to provide geo-information products designed for the detection, mapping, monitoring and forecasting of ground deformations, with emphasis on products useful to the Regional Civil Protection Department (Del Ventisette et al., 2013). All geographic information was projected using the WGS 84 projection datum and the Universal Transversal Mercator as coordinate system.

3.3. Product generation

The products delivered using the geodatabase were divided into two different categories: (i) basic products and (ii) advanced products. The former group includes products created using a single category of data (ancillary data or space-borne SAR data), whereas advanced products were generated combining the two categories. The quality of the

space-borne data was assessed before the product generation step in order to evaluate their usefulness and limitations.

3.3.1. Quality assessment of PS data

The PS detection suitability of the used PS datasets was evaluated considering the satellite parameters and the morphology of the study area, following the approach developed by Notti et al. (2010, 2014), which is a useful method to analyze the geometrical visibility of the area of interest. The suitability was evaluated by using two different indexes: the R-index (RI) and the land use (LU) index. The former represents the ratio between the slant range and the ground range (Notti et al., 2014) and provides the suitability of a given area to be investigated by a certain satellite system, taking into account the satellite parameters (incident angle) as well as the morphological characteristics of the slope (angle and orientation) derived from the available DEM. The LU index depends both on the land use and on the satellite sensor and PSI processing strategies (Notti et al., 2014). The RI ranges from the maximum value +1 to negative value. It assumes the maximum value when the suitability of the area to be investigated through the selected PS dataset is the highest. This means that the slope direction of the area is approximately parallel to the satellite LOS direction. On the contrary, the R-index assumes negative values, or around 0, when geometrical distortion effects prevent an acceptable visibility of the area. Considering the LU index and simplifying the land coverage of the test area, five land cover classes were defined: (i) urban built-up zones, (ii) rocky and debris areas, (iii) crops, (iv) forests and (v) water reservoirs.

3.3.2. Basic product generation

Part of the collected ancillary data such as the geological maps, land cover map, the pre-existing landslide inventory and the DEM derived products were used to produce the landslide susceptibility map (LSM) of the Messina Province. A simple implementation of Random Forest, a machine learning algorithm developed by Breiman (2001) that performs a multivariate classification, was developed in a Matlab environment in order to produce the LSM. The complete description of the methodology applied to LSM generation is reported in Catani et al. (2013). Numerous parameters were considered, in order to avoid the subjectivity in the choice of explanatory variables: elevation, curvature (general, planar, profile), slope, aspect, flow accumulation, Topographic Wetness Index (TWI), land use and lithology (Fig. 2). The source data are represented by a cell of 20 × 20 m: the average value inside a 100 × 100 m cell was calculated. For each parameter the standard deviation for numeric variables, and the variety for the categorical ones, were also calculated; always inside a 100 × 100 m window considering the variability of 25 cells (Lagomarsino et al., 2014).

Ground deformation velocity maps were obtained by using each interferometric dataset. In particular these maps consider the velocity measured along the LOS and, usually, they require an independent ground truth data validation (in situ measurements or observations). Following the methodology proposed in Notti et al. (2014) a stability

Table 1
Characteristics of the PSI datasets collected in the geo-database of the Messina Province.

Satellite	Area	Geometry	Temporal range	N° of images	N° of PS	PS/km2
ERS 1/2	Nebrodi	Ascending	23/08/1992–13/12/2000	138	43,405	23.22
ERS 1/2	Nebrodi	Descending	01/05/1992–08/01/2001	140	104,754	24.35
ENVISAT	Nebrodi	Ascending	22/01/2003–11/10/2010	107	137,770	38.07
ENVISAT	Nebrodi	Descending	07/07/2003–13/09/2010	98	99,175	32.46
RADARSAT-1	Nebrodi	Ascending	30/12/2005–26/01/2010	46	225,465	112.73
RADARSAT-1	Nebrodi	Descending	31/01/2006–03/02/2010	47	107,326	85.86
CSK	Nebrodi	Ascending	01/05/2011–03/05/2012	51	453,331	288.31
CSK	Nebrodi	Descending	16/05/2011–02/05/2012	64	793,725	729.94
TSX	Nebrodi	Descending	28/10/2011–22/09/2012	90	551,091	379.67
ERS 1/2	Peloritani	Ascending	08/09/1992–21/11/2000	48	6607	96.2
ENVISAT	Peloritani	Ascending	22/01/2003–20/05/2009	55	30,411	414.9

threshold (± 2 mm/yr) was used for the available C-band data. A more precautionary threshold was chosen for the X-band data (± 5 mm/yr) because of their higher standard deviation due to the shorter acquisition period (Table 1). These maps can be used at a regional scale.

Combining and integrating ground deformation velocity maps extracted by means of SqueeSAR technique with optical data (orthophoto, VHR optical satellite images and multi-temporal aerial photo), it was possible to highlight the presence of areas affected by high hydrogeological risk (hotspot mapping) at the local scale (Raspini et al., 2013).

3.3.3. Advanced product generation

Displacements and ground deformation velocities are measured by the satellite in the direction of the LOS whereas the real displacement actually occurs in three dimensions (Cascini et al., 2009). For this reason, a method to obtain a more reliable measured velocity is a key issue in landslide monitoring. The measured PS LOS velocities are projected along the steepest slope direction. The displacement is referred to the direction of the local maximum slope gradient, under the assumption that it is the most probable direction of real movement for a potential landslide phenomenon (Cascini et al., 2010; Notti et al., 2010; Plank et al., 2012; Bianchini et al., 2013; Herrera et al., 2013). In order to calculate the velocity projected along the slope (V_{slope} mm/yr), the formula proposed by Bianchini et al. (2013) and Notti et al. (2014) was adopted. This formula considers: (i) the slope and aspect derived from the DEM; (ii) and the satellite acquisition parameters (i.e. the azimuth, the incidence angle, the directional cosines: n_{los} , h_{los} , and e_{los} of the LOS). Thus, all the displacement velocities measured along the LOS (V_{los}) of all the available PS datasets were projected along the steepest slope, assumed (V_{slope}) as the most probable direction of movement. The V_{slope} velocity range is usually larger than V_{los} , since the minimum detected rate and the standard deviation are higher because of the major dispersion of the PS population. This method is useful when information acquired by different satellite sensors (with different LOS) and different acquisition orbits (i.e. ascending and descending) are available, in order to easily interpret and compare displacements projected along the same direction (steepest slope direction).

PS dataset can be profitably used to update an existing landslide inventory map. In particular, due to the acquisition parameters of the satellite systems (i.e. signal wavelength, revisiting time), this technique can only be applied to slow-moving landslide phenomena (Ciampalini et al., 2012) which according to Cruden and Varnes (1996) are classified as extremely slow (velocity < 16 mm/yr) and very slow (16 mm/yr $<$ velocity < 1.6 m/yr). Therefore those phenomena classified as “rapid erosion” and “rapid flow”, due to their high velocity, were excluded from the pre-existing database statistics analysis since they cannot be detected by satellite systems. Moreover, very small landslides (i.e., extension < 1 ha) were also removed from the database before

computing statistics. It is in fact almost impossible to have a minimum required number of 4 PS (Righini et al., 2012) located within a single landslide having such limited extension. The updating procedure was performed using a landslide activity matrix proposed by Righini et al. (2012). The state of activity assessment is based on the comparison between the mean velocity detected by the older available dataset and the one obtained using the more recent dataset.

PS datasets were combined with building maps at a municipality in order to produce building deformation velocity maps following the procedure proposed in Ciampalini et al. (2014). The deformation velocity of each building was calculated considering the average velocity of all the PS included in the building polygon. All the available C- and X-band datasets were used to monitor the evolution of the building deformation between the 1992 and 2012. A stability threshold of the building deformation between ± 1.5 mm/yr was chosen for the C-band data and ± 2 mm/yr for the X-band data.

The integration between space-borne and ground based SAR data was applied at a local (slope) scale in the Nebrodi area, for highly accurate monitoring and mapping activities on the landslide affecting the town of San Fratello, one of the most severely damaged urban centers after the winter 2010 event (Bardi et al., 2014). The GBInSAR employed system was designed and implemented by the Joint Research Centre (JRC) of the European Commission and its spin-off company Ellegi-LiSALab (Tarchi et al., 2003a,b; Casagli et al., 2009, 2010; Gigli et al., 2011; Di Traglia et al., 2014a,b). The radar system was installed at an average distance of 2100 m from the landslide. The area covered by a GBInSAR system depends on the distance between the sensor and the target, which is usually limited to a few hundreds of meters up to a few kilometers. In the specific case of San Fratello, the covered area is about 1 km², approximately corresponding to the landslide extension (Bardi et al., 2014). Cumulative displacement maps were obtained by means of a GBInSAR system dedicated to the monitoring of the February 14th 2010 landslide. The monitoring campaign was carried out from March 10th 2010 to March 14th 2013. Ground displacements were measured along the GBInSAR line of sight (LOS). The precision in the displacement measurement is 0.1 mm for punctual (few pixels) automatic extraction and displacement time series are obtained through the time differentiation of displacements obtained from two consecutive images (Di Traglia et al., 2014b). The integration of PS and GBInSAR approaches allows to overcome the physical limitations of each single technique, providing the displacement analysis of the same area from different points of view and in different temporal intervals.

Space-borne interferometric data combined with geological, geomorphological and hydrological data were used to refine the residual risk zonation mapping in areas affected by the 2009 event debris flows. Risk zonation was performed for built up areas using four different risk levels (Table 2) considering the proximity of past debris flow run out areas and of the riverbeds, building damages and presence of active slow moving landslides detected using PS data.

Table 2
Different levels of risk adopted for the risk zonation.

Risk level	Description
Level 0 – Green	Negligible geomorphological and hydraulic risk. Areas not affected by landslides. Population allowed to come back to their houses after the verification of the existence of access road and the functionality of services and basic infrastructure (water, electricity, sewage, etc.).
Level 1 – Yellow	Low geomorphological and hydraulic risk. Areas affected by landslides or areas nearby zones affected by landslides. Buildings can be used with some caution. Limited geotechnical and geomorphological stabilization works are required. Limited hydraulic mitigation works have to be performed. Civil Protection plans are required.
Level 2 – Pink	Medium to high geomorphological and hydraulic risk. Areas affected by landslides or areas nearby zones affected by landslides. Buildings can be used only after extensive stabilization works. Presence of buildings and infrastructures that may increase the geomorphological and hydraulic hazard. Building demolition and relocation cannot be excluded.
Level 3 – Red	Very high geomorphological and hydraulic risk. Areas close or within riverbed. Areas within landslides. In these areas buildings must be demolished to allow the restoration of pre-existing stream. In these areas, the structures (e.g., buildings) and/or infrastructure (e.g., roads) will be relocated to safer areas.

4. Results

4.1. Quality assessment of PS data

The R-Index was calculated for all the available radar datasets and classified into 5 classes. A good agreement between R-Index and PS density could be noticed: the better the R-Index is, the greater amount of PS and the greater PS density were detected. A general improvement of the RI from C-band sensors to X-band one was

observed, but among the C-band sensors RADARSAT-1 shows higher value with respect to ERS1/2 and ENVISAT (Fig. 3). The inversion between the highest and lowest RI values related to the orientation of the slopes was observed in all the datasets acquired both in ascending and descending geometry (ERS 1/2, ENVISAT, RADARSAT-1 and CSK). Thus, when comparing ascending and descending passes of the same satellite, it can be observed that the highest and the lowest R-Index classes are basically inverted on slopes facing E and W (Fig. 3). It is worth highlight that the Messina Province area is particularly suitable

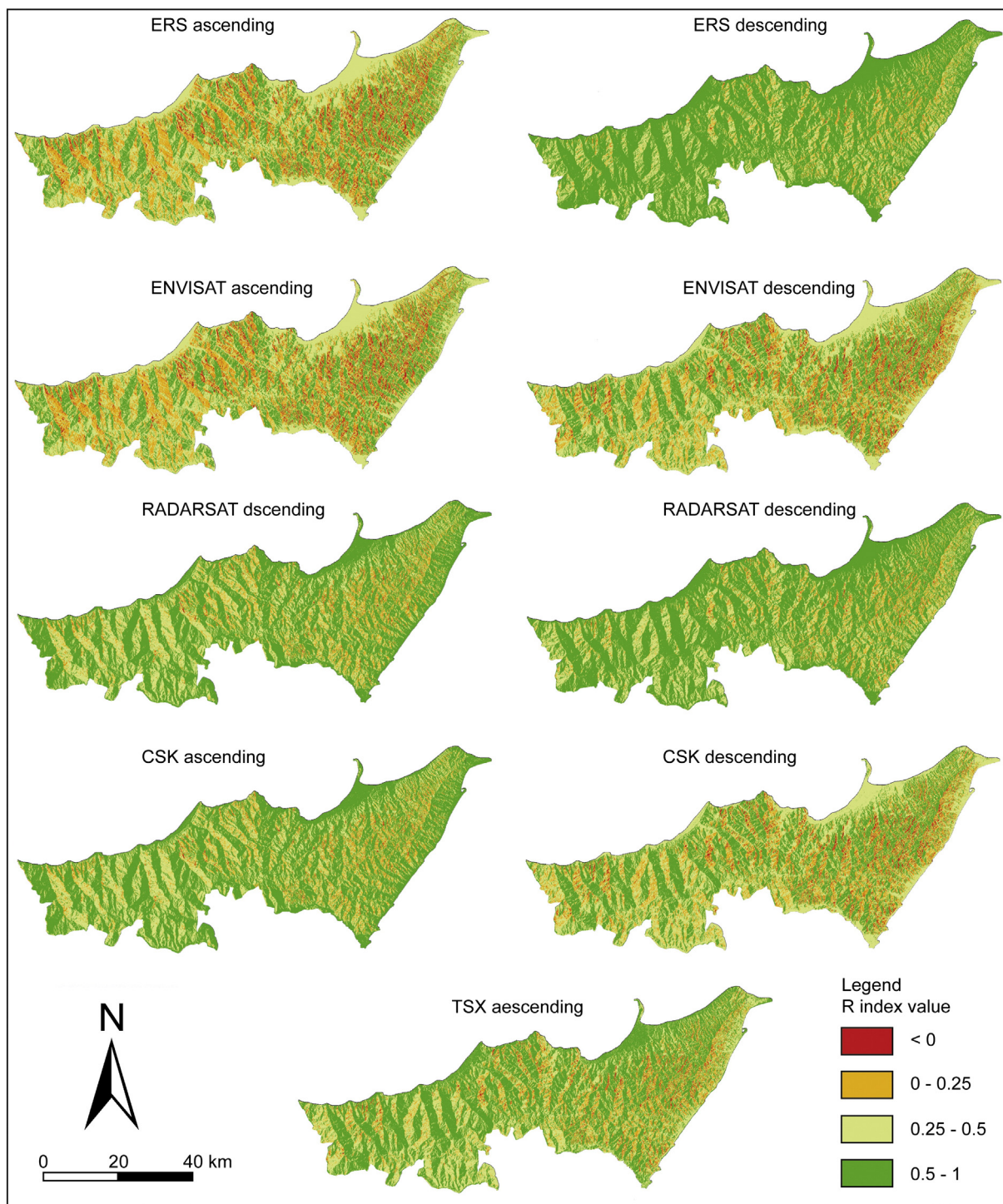


Fig. 3. RI distribution for the Messina Province considering the acquisition parameters (incident angle) of each satellite and the morphology of the study area (slope, aspect). The RI ranges from the +1 to negative value assuming the maximum value when the morphology of the area is optimal to be investigated through the selected PS dataset. (See online version for color images).

for this relief visibility analysis because it is characterized by the presence of N–S oriented valleys with E or W facing slopes. The enhancement of the RI can be related to the differences in the incident angle, since the greater is the incidence angle, the greater is the R-Index. The average PS density is higher for the X-band sensors because of their higher resolution, which allows the detection of a greater amount of radar benchmarks. ERS 1/2 and ENVISAT show the higher number of PS in the 0.25–0.50 class, whereas RADARSAT-1 and X-band sensors (CSK and TSX) reveal a greater PS amount in classes characterized by higher value of the R-Index.

The evaluation of L-index deals with the PS number on land use, which depends on the types of land coverage of the area and on their characteristics of maintaining the scattering properties in time, as well as on the diverse microwave band data acquired by different satellite sensors. Areas with buildings and structures are characterized by the highest PS densities. In these areas the presence of human made structures, corresponding to the most stable reflectors, increases the PS density for both the acquisition bands (C- and X-bands). Large rock and talus outcrops can be considered as good stable reflectors too, showing good PS densities, especially in X-band. Water reservoir areas show high PS density because they correspond to seasonal streams which are dry for most part of the year. During the dry season, the river beds are formed by blocks corresponding to stable PS.

4.2. Basic products

4.2.1. Landslide susceptibility map

The landslide susceptibility map of the Messina Province (Fig. 4) shows that most of the analyzed area is affected by moderate to very high landslide susceptibility. Most of the areas scarcely affected by ground deformation phenomena are located along the coast, in correspondence with the narrow coastal alluvial plains. The map also shows that the Nebrodi Mountains are more susceptible than the Peloritani Mountains. The performance of the model used was evaluated by building a ROC (Receiver Operating Characteristic) curve, shown in Fig. 4. The AUC (Area Under Curve) value of 0.73 highlights a good result.

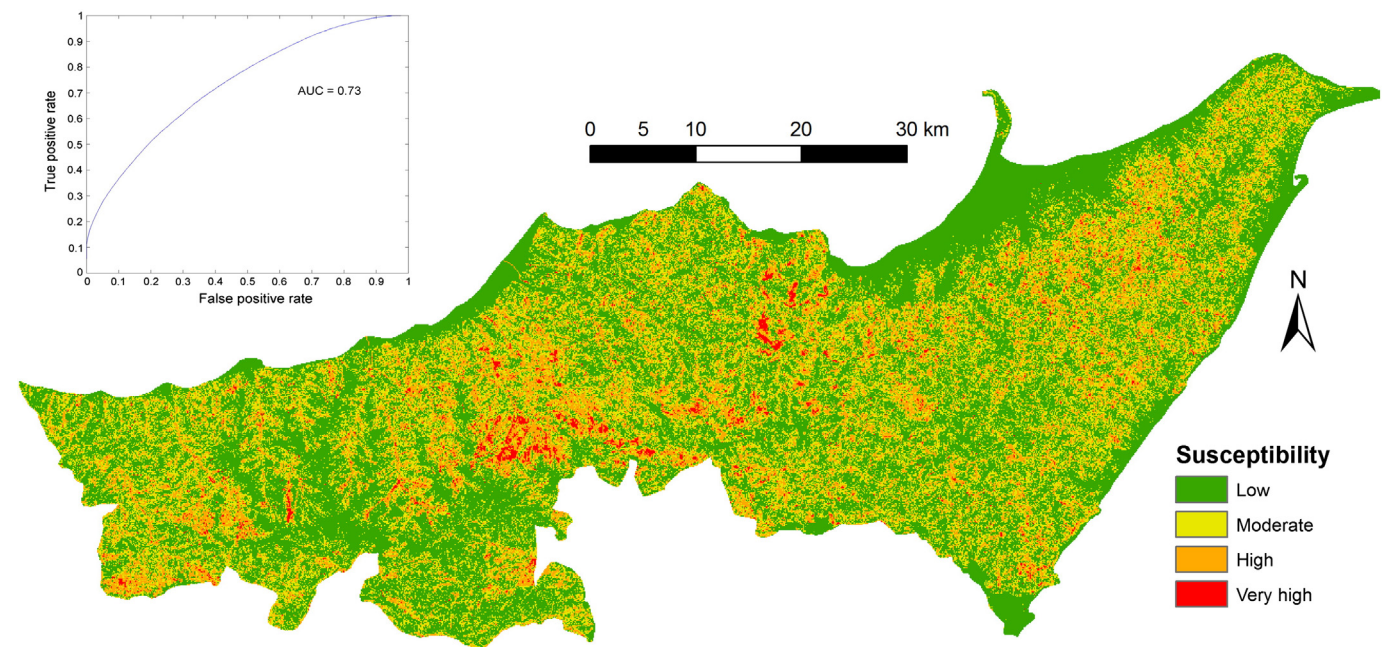


Fig. 4. Landslide susceptibility map derived from the available ancillary data (elevation, curvature, (general, planar, profile), slope, aspect, flow accumulation, TWI, land use and lithology) included in the Messina Province geo-database and the related ROC curve. The susceptibility map was produced using a simple implementation of Random Forest. (See online version for color image).

4.2.2. Ground deformation velocity maps

Ground deformation velocity maps (Fig. 5) can be used at regional scale in order to detect the most unstable areas. These maps can be elaborated clustering unstable and stable PS in order to determine active and stable areas. This kind of map is very useful in regional studies because most unstable areas can be easily and immediately detected allowing the attention to be focussed on specific targets. The comparison among PS dataset acquired in different time intervals can be used to evaluate the evolution in time of the areas affected by slow moving ground deformation phenomena.

4.2.3. Giampilieri area hot spot mapping

The abovementioned approach can be performed also at a local scale. Following the autumn 2009 event previously described, a multi-temporal analysis of satellite radar images, processed through the SqueeSAR algorithm, was exploited for detecting and mapping slope instability at basin scale in the south-western part of the Messina Province. Available PS data provided estimates of yearly deformation velocity, referred to both historical (1992–2001; ERS 1/2 data) and recent (2003–2009; ENVISAT data) scenarios. The investigated area, with an extent of about 75 km², is located in a narrow coastal area south of the suburbs of the city of Messina, delimited by the Ionian sea on the East side and by the Peloritani ridge on the West side. The area includes the following five municipal towns, located in the Messina district: Ali, Ali Terme, Itala, Scaletta Zanclea and Messina. The hotspot mapping procedure identified 26 sites (Fig. 6) characterized by high hydrogeological risk (Raspini et al., 2013). On the basis of available multi-interferometric data, these sites were assessed as the most critical in terms of hydrogeological hazard and risk, for the type and extent of the detected landslide phenomena, for the measured deformation velocities and for the presence of elements at risk (Fig. 6). For each site, a PS landslide mapping was performed and validated through field surveys, and the updating of the pre-existing landslide inventory. A validated hotspot analysis (Altolia village, site number 14 in Fig. 6), representative of the type phenomena identified in the whole study area, is presented. Fig. 7 shows the results from photo and radar interpretation for Altolia, a village in the Messina municipality with 460 inhabitants. The settlement has developed along the right bank of

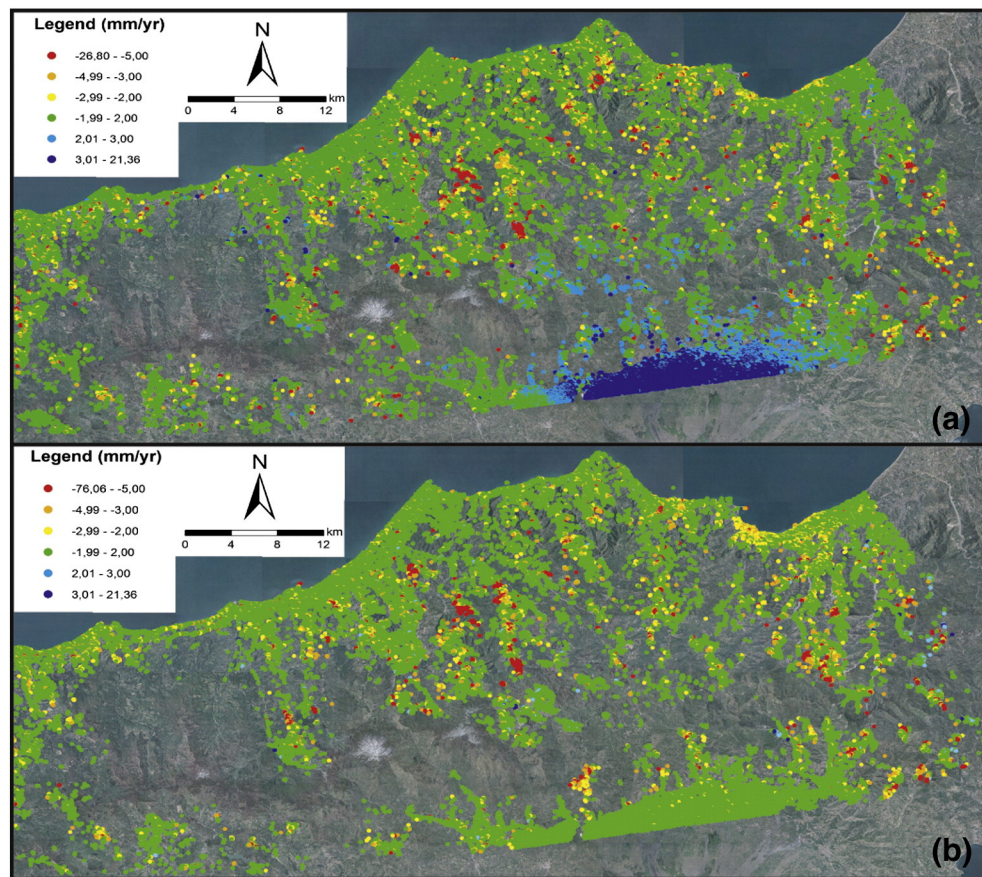


Fig. 5. Example of ground deformation velocity maps obtained through (A) ascending ERS1/2 (1992–2001), (B) ascending ENVISAT (2003–2010). The area characterized by a cluster of blue PS in (A) corresponds to the northern sector of the Etna volcano. (See online version for color images).

Giampileri river. An overview of the SqueeSAR results, expressed in mm/yr, both for ERS 1/2 and ENVISAT datasets is shown in Fig. 7a and b. The PS results highlighted ground motion displacements in both historical (1992–2001; ERS 1/2) and recent (2003–2009; ENVISAT) scenarios. In particular, available datasets allowed the identification of a large sector in the southeastern part of the village characterized by displacements with an average velocity ranging from 2 mm/yr to 10.7 mm/yr in the ERS 1/2 dataset, and from 2.2 mm/yr to 8.9 mm/yr in the ENVISAT dataset. Photo interpretation of stereoscopic color images (1:3500 scale) and field surveys allowed the detection and mapping of a large active continuous slide affecting the south-eastern part of Altolia village (Fig. 7c). During the field campaign, carried out in the framework of the post-disaster activities and aimed at validating SqueeSAR results, several effects on infrastructure (building cracks and damage) were detected. A detailed study of landform features (scarps, counterscarps, tension cracks) led to a complete characterization of the Altolia landslide, which could be divided in different sectors characterized by homogenous morphologic behavior (crown and accumulation zone).

4.3. Advanced products

4.3.1. V_{Slope} ground deformation velocity maps

A more accurate evaluation of the deformation velocities at the local scale was performed converting LOS velocities into V_{Slope} velocities combining the ground deformation velocity maps and the Messina Province 20×20 m DEM. The V_{Los} projection along the local slope leads to a significant reduction of the PS population (Notti et al., 2014): PS amount with V_{Slope} velocities was reduced for ERS 1/2 dataset to the 38% of the V_{Los} PS amount. For ENVISAT dataset, PS population was reduced to the 42%. V_{Slope} RADARSAT-1 is the 43% of the PS V_{Los} .

Within CSK dataset, V_{Slope} dataset is the 22% of V_{Los} population. TSX PS V_{Slope} were the 84% of the V_{Los} population. This loss of information in terms of PS amount was compensated by the more reliable evaluation of the ground deformation using the V_{Slope} instead of the V_{Los} . According to the combination of the local topography (including aspect and gradient of the slopes) with the acquisition geometry of the satellite, some movements within landslide boundaries seemed to be uplift motions since they revealed a movement toward the satellite sensor. This misunderstanding interpretation can be partially solved by conversion to V_{Slope} values, that allows observing the movement in agreement with the real expected displacement down the slope, and thus permits a more reliable and robust analysis of the slope dynamics.

4.3.2. Updated landslide inventory map

The updated landslide inventory map (LIM), obtained by combining the pre-existing landslide inventory (PAI, 2012) and PS datasets, was performed in a test area (25 km^2) located in the western part of the Messina Province. The PAI is dated up to 2012 and includes landslide phenomena classified with respect to the typology and the state of activity (active, dormant, inactive – including relict and abandoned phenomena – and stabilized), according to a simplified version of Cruden and Varnes (1996) classification. The updated LIM was realized using the following satellite SAR datasets, RADARSAT-1 (2005–2010) and CSK (2011–2012), both acquired in ascending and descending geometries. The procedure applied allowed the identification of new landslides, modifying their boundaries and assessing the state of activity following the Cruden and Varnes (1996) classification. The assessment of the state of activity was based on the comparison between the mean velocity detected by the older available dataset (RADARSAT-1 in this case) and that obtained using the more recent one (CSK). The results obtained showed an increase in the accuracy of the updated

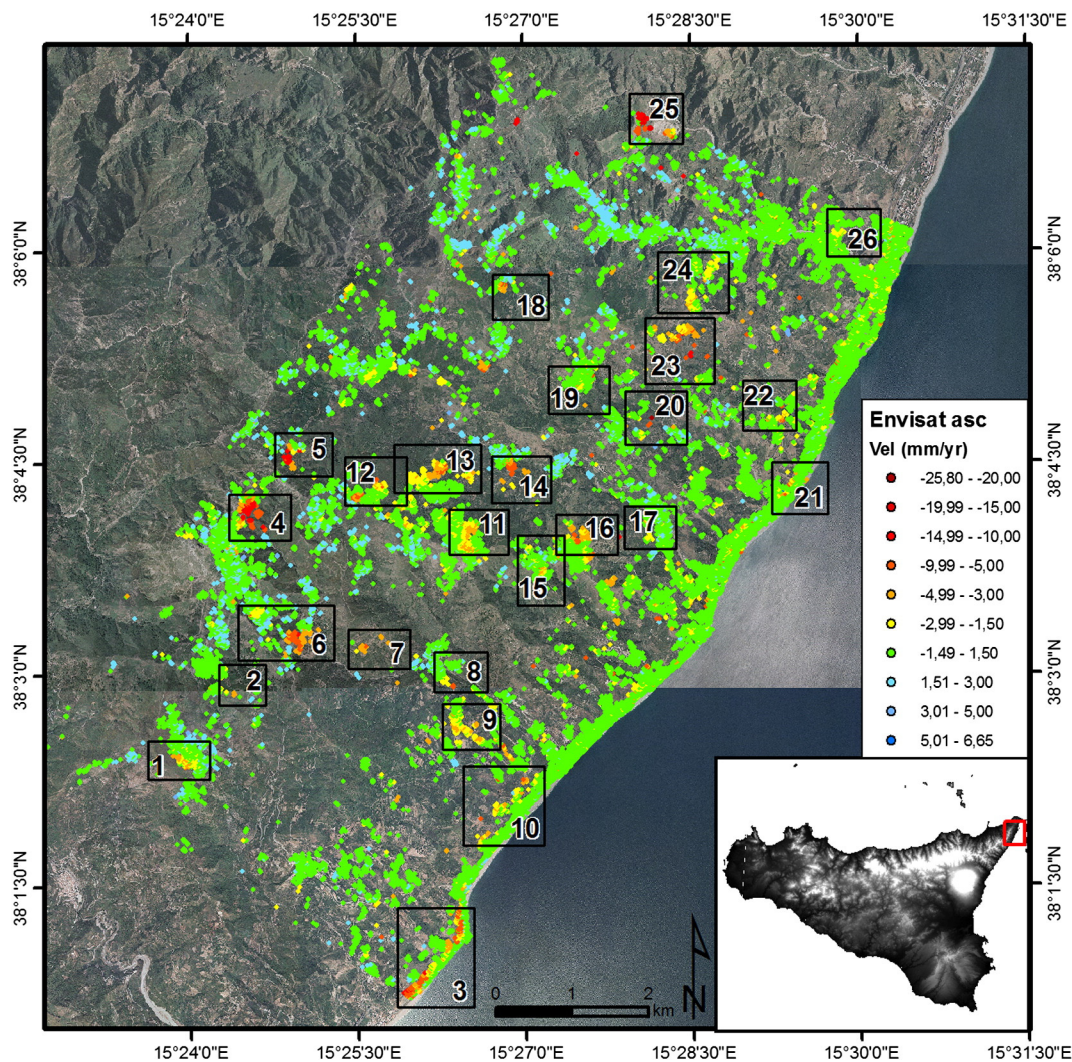


Fig. 6. Location of the 26 sites characterized by high hydro-geological hazard (hotspot mapping). 1) M. Santo; 2) P.le Puzzu; 3) Ali Terme; 4) P.le Seddiri; 5) P.le Cimmario; 6) P.le Pitarra; 7) Culma Caravagi; 8) Itàla; 9) Croce; 10) Itàla Marina; 11) M. Pietralunga; 12) P.le Lanzaro; 13) P.zzo Scapola; 14) Altolia; 15) Monticeddu; 16) P.le Laridda; 17) Giampileri; 18) P.le Dinareddi; 19) Pezzolo; 20) Briga Superiore; 21) San Paolo; 23) Upper Schiavo river basin; 24) S. Stefano; 25) P.le Furcu; 26) and Villa Parotta. These areas were selected for the presence of clusters of PS characterized by the highest ground deformation velocities. (See online version for color image).

LIM with 25 new detected phenomena (13.16%) and the enlargement of other 35 landslides (18.42%).

4.3.3. Building deformation velocity map (San Fratello)

Buildings are sensitive to movements caused by landslides. The assessment of the building deformation in landslide area, using the PS datasets, represents a useful tool in order to understand the landslide evolution, magnitude and stress distribution. This method can be applied both in a municipality affected by past landslides, monitoring residual movements, and in other areas detected as unstable, by means of the hotspot mapping, but not yet involved in slope instability phenomena. Furthermore, the building deformation velocity maps obtained, which are valuable products to monitor the safety of urban areas affected by ground deformation, can be easily validated through dedicated field surveys devoted to the detection and evaluation of building damage. The designed geodatabase was used to monitor the evolution of the building deformations that occurred between the 1992 (ERS1/2) and the 2012 (CSK) in the San Fratello Municipality, generating different building deformation velocity maps. The maps produced (Fig. 8) clearly show an increase in the number of buildings affected by deformation phenomena measured after the 1992 but before the event of the large landslide that occurred on February 14th 2010. The pre-event data highlight deformation also

along the western slope of the town, affected by a historical landslide that occurred in 1922, detecting slow but continuous deformation. The most interesting results were obtained using the CSK dataset acquired during the post event phase. The related building deformation velocity map highlights the presence of important residual deformations in the areas most intensely damaged during the 2010 landslide (Fig. 8b).

4.3.4. Local deformation analysis (San Fratello)

In the town of San Fratello a detailed local deformation analysis was performed combining space-borne and GBInSAR data (Fig. 9). Cumulative displacement maps were used to identify areas characterized by different ground motion. The peak deformations were located in correspondence with the western landslide boundary (Fig. 10). Ground deformation in these areas was evaluated also using the space borne data acquired along different LOS with respect to the GBInSAR system.

The C-band data acquired between 1992 and 2010 were used to evaluate the potential risk of the area. X-band and GBInSAR data were acquired to monitor ground deformation during the post event phase. The combined space borne (both C- and X-band) and GBInSAR analysis was performed in order to refine the landslide boundary. With respect to the landslide boundary, assessed by means of a geomorphological field survey carried out by the Sicily Region Civil Protection Department

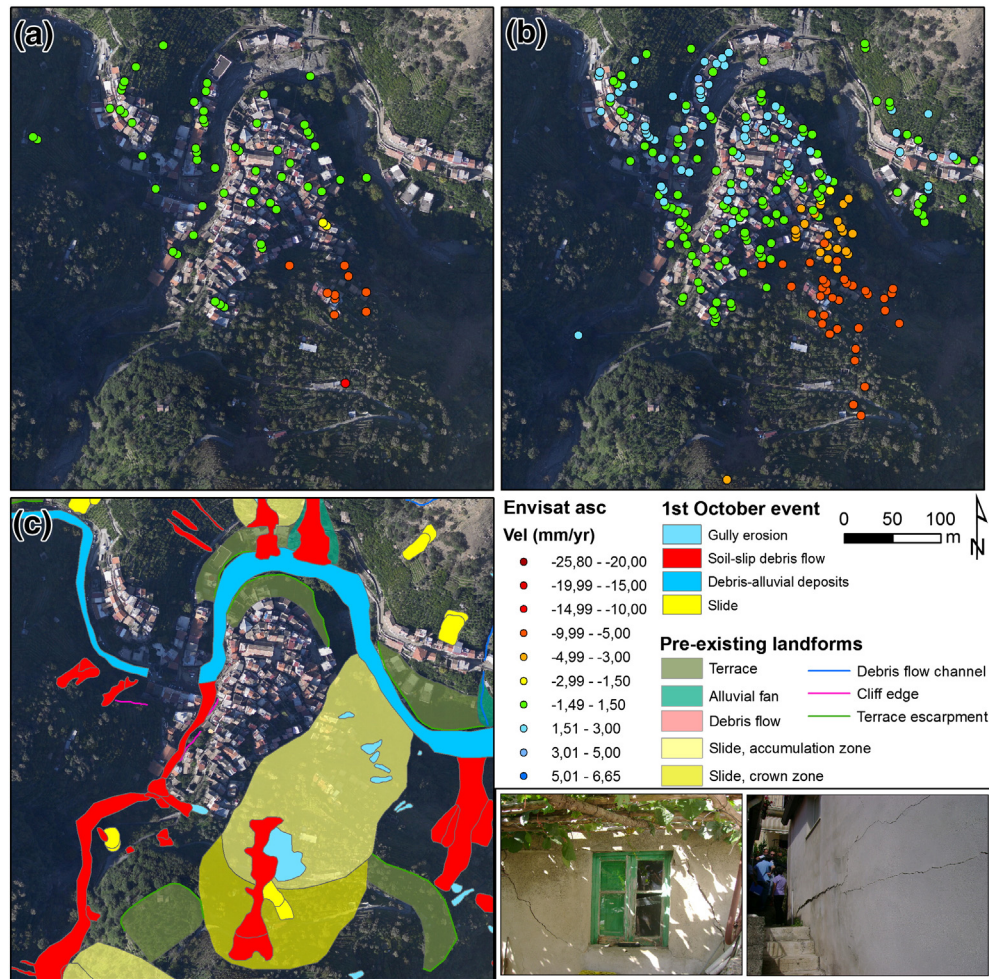


Fig. 7. The Altolia (Messina) hotspot. (a) ERS dataset; (b) ENVISAT dataset; and (c) geomorphological map where the landforms were divided into pre-existing and formed after the 1st of October event. PS datasets clearly suggest that the biggest landslide located in the southeastern sector is active at least since 1992. (See online version for color images).

(DRPC), the analysis of the available SAR data highlighted areas affected by deformation located also outside of the landslide perimeter, suggesting that the latter was slightly underestimated (Fig. 10).

The integration between space-borne and ground-based data was useful to analyze the ground deformation related to the San Fratello landslide in different time intervals (from 1992 to 2013) and with different LOS and ground resolutions. The new landslide boundary contains areas affected by deformation, which were detected by the C-band sensors during the pre landslide event phase, and by both the COSMO-SkyMed satellite and the GBInSAR system during the post-event phase. The new landslide area increased in extension from 1 to 1.2 km², and was validated also through field surveys aimed at the buildings and infrastructures damage assessment.

The accuracy obtained in landslide mapping and monitoring in correspondence of a large inhabited area affected by slope instability, such as the town of San Fratello, proved to be crucial in risk management activities and in the preparation of emergency plans.

4.3.5. Residual risk zonation (Altolia)

Immediately after the 1st of October event, a microzoning of landslide risk was performed for all the populated centers affected by landslide phenomena. The purposes of the microzoning were (i) to prioritize risk mitigation works and (ii) to identify areas characterized by low to null risk. As an example, the case of the zonation of Altolia is presented and discussed. This case is particularly relevant because it includes both the residual risk related to occurrence of fast moving debris flows and a slow moving pre-existing slide. The populated center is classified

according to four zones with different risk levels (Table 2). Most of buildings and houses close to the two riverbeds (Giampilieri and its right-bank tributary the Mandarina, Fig. 10) were classified with different level of risk (from 1 to 3) when several mud, earth and debris flows occurred. These phenomena were triggered as a consequence of the high water content of the soil located on the slopes of the Mandarina creek. The mobilized material moved as a channeled flow within the creek, damaging the buildings on the left and right banks, and finally flowing through a culvert, into the Giampilieri creek. Following the ranking displayed in Table 2, these buildings were classified in the highest risk level both for their location (inside or close to the riverbed) and for their damage degree. The southeast part of the village was classified as medium to high risk (level 2) even though it was not affected by debris- or mud-flow phenomena. This level of risk was due to the presence of a slow-moving pre-existing slide, whose presence was inferred from the analysis of radar data, photo interpretation and field survey. The central part of the village, located on the hilltop, far from the riverbeds, is characterized by negligible geomorphological and hydrological risk. Furthermore PS data highlight that this area is not affected by slow-moving landslide phenomena (Fig. 10).

5. Discussion

Each product presented in this paper for landslide territorial management shows both advantages and limitations, which can be enhanced or reduced by choosing the appropriate scale of application, geomorphological/geological background or typology of phenomenon.

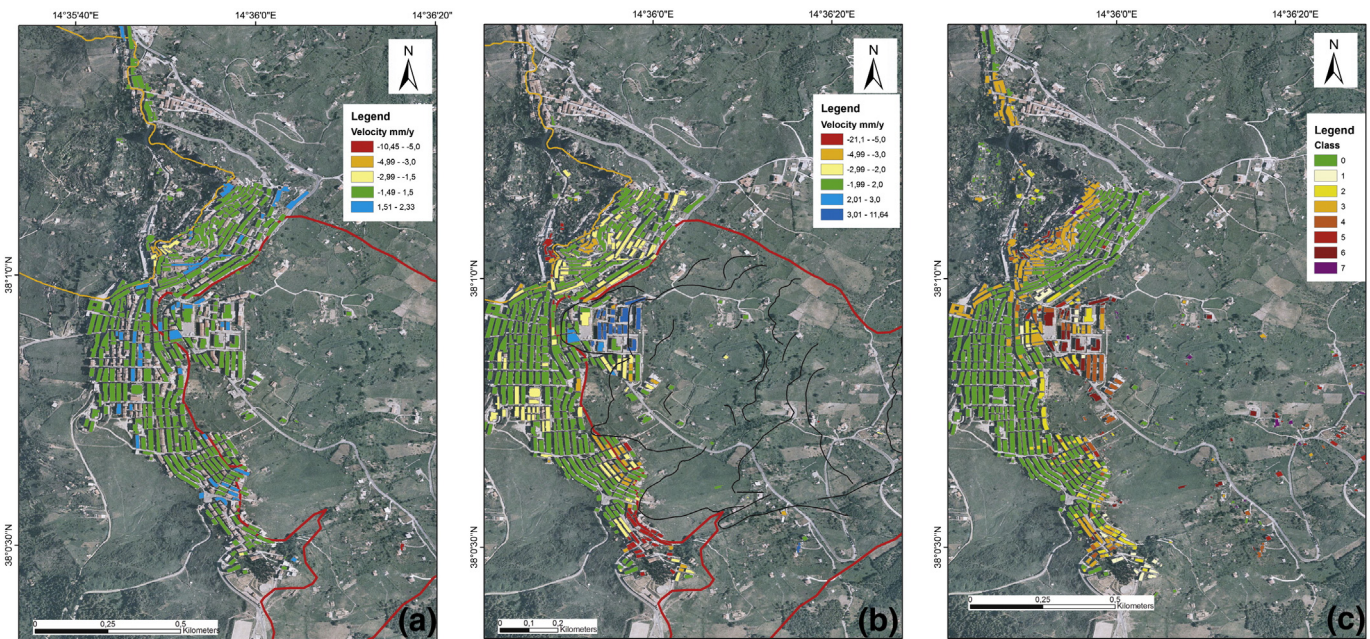


Fig. 8. Examples of building deformation velocity maps: (a) building deformation velocity map by using the ENVISAT dataset; (b) building deformation velocity map by using the CSK dataset; and (c) damage assessment map of San Fratello. The red line in (a) and (b) represents the 2010 landslide boundary. The black lines in (b) represent the main scarps developed after the 2010 landslide. It is worth noting that most damaged buildings (c) correspond to buildings affected by the highest deformation velocity measured by CSK data (b) suggesting that after almost 2 years from the main event the area is still subjected to residual deformations. (For interpretation of the references to color in this figure legend, the reader is referred to the web version of this article.)

For example all the products based on PSInSAR data (ground deformation velocity maps, hotspot mapping, V_{Slope} projection, updated LIM, building deformation velocity map and partially the risk zonation mapping) were affected by the limitations of this technique. The most significant limits of PSInSAR data mainly refer to the different technical parameters of the satellite systems used, which result in unlike acquisition features and consequent results (Ferretti et al., 2001). The presently available SAR data, from both historical archives and currently operational missions, do not allow the measurement of deformations faster than few tens of cm per year (Hanssen, 2005; Crosetto et al., 2010).

Velocities compromising the PS processing depend on the employed SAR wavelengths and on the satellite repeat cycles; these recorded displacement rates resulted: (i) from about 15 cm/yr up to 20 cm/yr in C-band (for ERS/ENVISAT and RADARSAT satellites, respectively); (ii) about 25 cm/yr for TerraSAR-X; (iii) 68 cm/yr for COSMO-SkyMed system with 4 operating satellites in X band. Consequently, rapid surface movements characterized by higher motion rates could not be correctly detected and analyzed. Another limit affecting the multi-frequency PS data is the possibility to improve detection and monitoring of hydrogeological events not in real-time, but only mainly in the

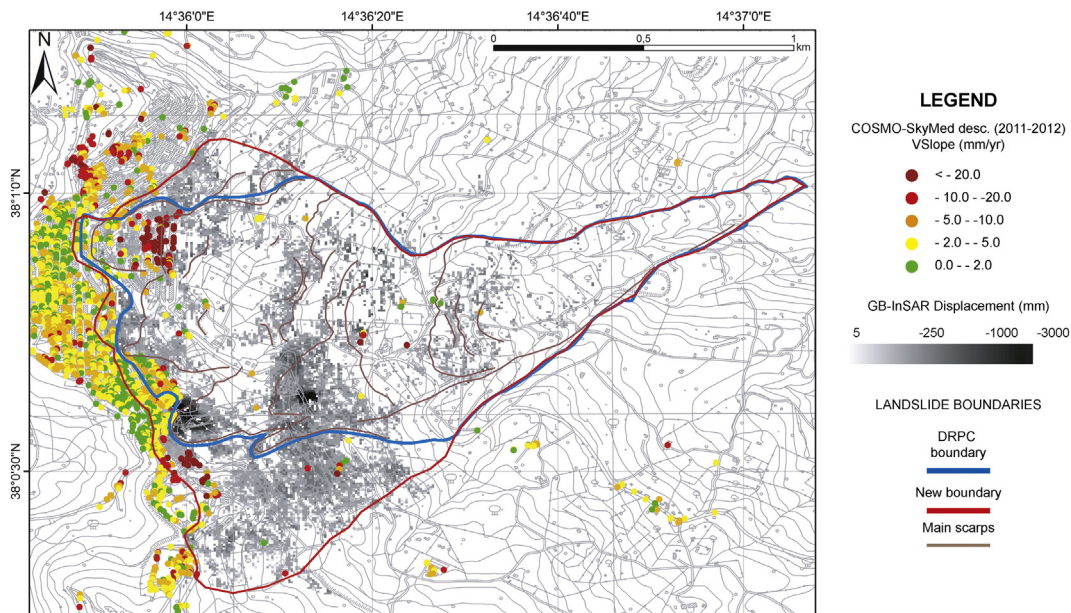


Fig. 9. Integration between space borne (CSK) and GBInSAR measurement. Comparison between the DRPC landslide boundary, obtained through field investigation, and the new boundary inferred by the integration between PS and GBInSAR data. On the background: the GBInSAR cumulative displacement map (from March 2010 to March 2013) and the COSMO-SkyMed data (from Bardi et al., 2014). (See online version for color image).

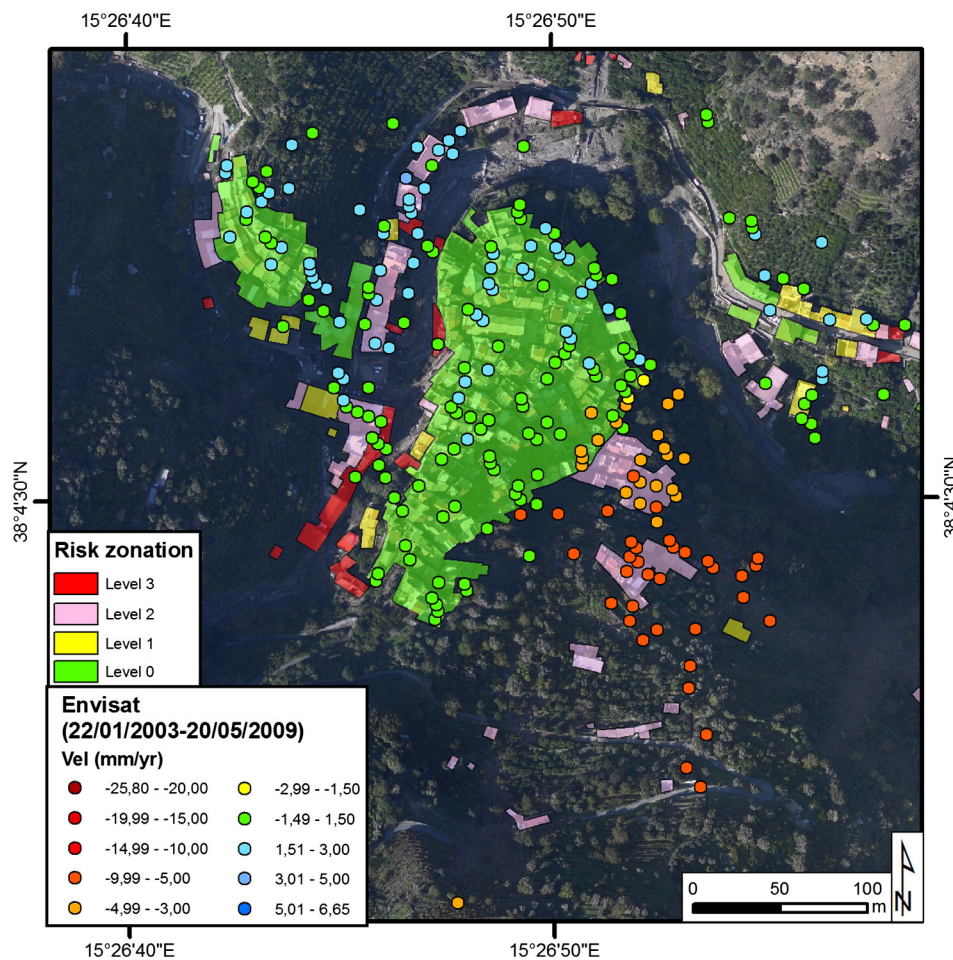


Fig. 10. Landslide risk zonation for the Altolia village (Messina). The four risk levels were decided following the description of Table 2 considering buildings characteristics (damages and distance from the riverbed) and the detected ground deformation velocity by SAR sensors. Light blue arrows correspond with the main flow directions of the Giampileri and Mandarina creeks. (For interpretation of the references to color in this figure legend, the reader is referred to the web version of this article.)

deferred time, and, partially, in the near- real time. By contrast, this approach allows the analysis of the temporal evolution of ground deformation up to 1992 (in case of ERS-1/2 satellite imagery availability). Concerning the PS spatial sampling, vegetation causes decorrelation in SAR images, while stable scatterers coincide with rocky outcrops and man-made built-up structures (Werner et al., 2003). Thus, while in some areas, like urbanized zones, PS interferometry obtains a reasonably good sampling, in other areas (vegetated, rural and forested) benchmarks are very reduced and PS interferometry tends to systematically fail. This is particularly true when using higher frequencies (e.g. C-band), whereas lower frequencies (e.g. L-band sensors) are less affected by atmospheric absorption, less attenuated by the vegetation canopy, providing a higher number of PS.

The PSInSAR technique allows the measurement of slow and very slow ground deformation (up to few millimeters per year) representing a useful support technique for landslide hazard mapping and monitoring activities, detecting movements that can occur several weeks or months before a catastrophic failure (Bardi et al., 2014). This technique can be used both at the regional or local scale.

The limitation related to the PSInSAR technique can be solved or reduced by integrating its results with those obtained through other techniques and available data. For example, at the local scale, the ground deformation velocity can be assessed more frequently in time using a ground based interferometer which can acquire on routine displacement data. A geodatabase makes easier the integration among different techniques and data, often represented by geographic

information (thematic maps, field measurements, remote sensing measurements).

The availability of a geodatabase integrating data and products strictly devoted to landslide hazard represents a great support for the public authorities in charge of landslide risk management (Pagliara et al., 2014). The opportunity to obtain a framework as complete as possible and continuously updated with new products and data organized in a geodatabase facilitates the utilization of all the available information in each phase of the emergency cycle, both in real and in deferred time.

The geodatabase structure and its workflow to produce each product were shared and discussed with public authorities and users at different administrative levels (national, regional and local), which were potentially involved in landslide risk management activities. This close collaboration among scientists, stakeholders and users was useful to make the scientists and researchers able to provide products and disseminate these with a geodatabase, meeting the user needs, both in terms of value added of the products and of their accessibility. The availability of all the data used to generate the basic and advanced products supports the users to understand the specific product value and their usefulness of application. In addition, the validation of the products and the structure of the geodatabase and the pre-operational application were useful to integrate the results in the operative workflow and in the most useful ways. The challenge to continuously update the geodatabase with new products and to increase the usability of its structure will allow satisfying new user requirements. This will make

this work useful and suitable to be developed and built in other test sites in order to aim at the geodatabase and product availability with the same quality at national level.

In Table 3 the landslide product integration performed in the Civil Protection emergency cycle is outlined, particularly regarding the technical assessment process implemented by the close collaboration of research institutes and public authorities. The technical assessments obtained were inputs for the user technical activities.

Products obtained through the geodatabase of the Messina Province are currently used by the authorities during the different Civil Protection phases. For example, a combined use among the updated landslide inventory map, the ground deformation velocity maps and the susceptibility map is useful for prevention and preparedness actions. These products highlight the most unstable areas and the degree to which an area can be affected by future slope failure at the regional scale. These information allow to decide the priority for the definition of the Civil Protection emergency plan for the most hazardous areas.

Local scale products (e.g. residual risk zonation, hotspot mapping, updated landslide inventory map) are more useful during the emergency phase to plan the preliminary stabilization interventions, an early warning system and the evacuation of the population. These products were successfully used for the Giampilieri and Altolia emergency and evacuation plan. The management of the recovery phase needs products useful to monitor the landslide area and to plan preliminary interventions. During this phase products such as residual risk zonation, local scale deformation analysis (using the GBInSAR or field measurements) and the building deformation velocity maps are of fundamental importance. These products and activities were used to monitor the San Fratello landslide and to make people and workers' activities safe.

The products generated after a landslide emergency event will become the starting point for the next prevention and preparedness phase.

6. Conclusions

Ground deformations, and in particular landslides, represent one of the most hazardous phenomena that cause economic and human losses. For these reasons Civil Protection and local authorities are strongly interested in assessing the analysis of the spatial distribution of landslide hazard and risk, for planning and decision-making activities, and in particular for a proper management of the different Civil Protection cycle phases (preparedness/prevention, emergency and recovery). Updated landslide inventory maps provide useful information on location, occurrence, landslide-type, area involved, state of activity, failure mechanisms, triggering factors, and damage assessment. These tasks require a very large amount of information, such as the detection

and mapping of unstable areas, thematic and environmental data, and element at risk evaluation.

Detection and mapping of unstable areas are essential procedures that can be produced and updated by handling different data in a dedicated geodatabase where available geographic information and new acquired remote sensing data (earth observation, ground based, aerial) can be profitably exploited to improve the quality of landslide inventory maps, landslide assessment and susceptibility.

In this work, a geodatabase of the Messina Province is presented and described highlighting the capability of the GIS environment to obtain useful products for the management of the landslide-induced hazard. The geodatabase contains available ancillary data and new acquired SAR and optical data, which were used to produce regional and local maps useful for the Civil Protection Department to manage the 2009 and 2010 events post emergency phases. For example the building deformation velocity maps produced in San Fratello and the risk zonation realized in Altolia were used to plan recovery intervention and urban development. The geodatabase was also used to produce ground deformation velocity maps and the susceptibility map of the Messina Province, which can be used to detect the most unstable areas for the planning of mitigation activities. The structure of the database allows the updating of some of the products presented in cases of acquisition of new data, thus providing continuously updated maps.

The presented database was designed following the requirements of the local and national Civil Protection authorities which today constantly use it to manage the landslide hazard of the Messina Province at regional and local levels. This work proves that a very complete geodatabase is a flexible tool suitable to contribute to the management of the landslide hazard and risk.

Acknowledgments

The research leading to these results received funding from the European Union Seventh Framework Programme (FP7/2007–2013) under grant agreement No. 242212 (Project DORIS). This study was funded by the Seventh Framework Programme of European Commission: Landslide Modelling and Tools for vulnerability assessment preparedness and recovery management (LAMPRE). Federico Di Traglia is supported by a post-doc fellowship funded by the Regione Toscana (UNIFI-FSE) under the project RADSAFE (UNIFI-4) in the framework of the research agreement between DST-UNIFI, DST-UNIFI and Ellegi-Lisalab. The risk zonation for the village of Altolia has been performed in collaboration with the National Civil Protection and the Department of Civil and Environmental Engineering of the University of Catania. We thank two anonymous reviewers and the editor for their suggestions which greatly improved this work.

Table 3
Applications of landslide products in the Civil Protection emergency cycle.

Civil Protection phase	Landslide products	Technical assessment	User technical activities
Prevention and preparedness	- Landslide inventory map - Ground-deformation velocity map - Susceptibility map	- Definition of landslide hazard scenarios	- Definition of the hydrogeological management plan - Definition of Civil Protection emergency plan
Emergency	- Event and pre-existing Landslide inventory map - Residual risk zonation - ground deformation velocity map - Hot spot mapping	- Residual risk evaluation - Displacement monitoring - Evaluation the magnitude of the landslide event - Plan of the preliminary stabilization interventions	- Early warning - Evacuation - Relocation - Adoption and/or updating of civil protection emergency plan
Recovery	- Ground-deformation velocity maps - Landslide inventory maps - Residual risk zonation - Susceptibility map - Projected ground deformation velocity map - Local scale deformation analysis - Building deformation velocity map	- Evaluation of the preliminary stabilization interventions - Plan of the final stabilization interventions - Updating of landslide hazard scenarios - Evaluation of local geomorphological hazard for relocated settlements	- Adoption of the preliminary stabilization plan - Updating (if necessary) of the preliminary stabilization plan - Adoption of the final stabilization plan - Updating of the hydrogeological management plan - Updating of the Civil Protection emergency plans

References

- Ardizzone, F., Basile, G., Cardinali, M., Casagli, N., Del Conte, S., Del Ventisette, C., Fiorucci, F., Garfagnoli, F., Gigli, G., Guzzetti, F., Iovine, G., Mondini, A.C., Moretti, S., Panebianco, M., Raspini, F., Reichembach, P., Rossi, M., Tanteri, L., Terranova, O., 2012. Landslide inventory map for the Briga and the Ciampalini catchments, NE Sicily, Italy. *J. Maps* 8, 176–180.
- Bardi, F., Frodella, W., Ciampalini, A., Bianchini, S., Del Ventisette, C., Gigli, G., Fanti, R., Moretti, S., Basile, G., Casagli, N., 2014. Integration between ground based and satellite SAR data in landslide mapping: the San Fratello case study. *Geomorphology* 223, 45–60.
- Battistini, A., Segoni, S., Manzo, G., Catani, F., Casagli, N., 2013. Web data mining for automatic inventory of geohazards at national scale. *Appl. Geogr.* 43, 147–158.
- Bellotti, F., Bianchi, M., Colombo, D., Ferretti, A., Tamburini, A., 2014. Advanced InSAR Techniques to Support Landslide Monitoring. In: Pardo-Igúzquiza, E., Guardiola-Albert, C., Heredia, J., Moreno-Merino, L., Durán, J.J., Vargas-Guzmán, J.A. (Eds.), *Mathematics of Planet Earth, Lecture Notes in Earth System Sciences*. Springer, Berlin Heidelberg, pp. 287–290.
- Bianchini, S., Herrera, G., Notti, D., García-Moreno, I., Mora, O., Moretti, S., 2013. Landslide activity maps generation by means of Persistent Scatterer Interferometry. *Remote Sens.* 5, 6198–6222.
- Bianchini, S., Ciampalini, A., Raspini, F., Bardi, F., Di Traglia, F., Moretti, S., Casagli, N., 2014a. Multi-temporal evaluation of landslide movements and impacts on buildings in San Fratello (Italy) by means of C-band and X-band PSI data. *Pure Appl. Geophys.* <http://dx.doi.org/10.1007/s00024-014-0839-2>.
- Bianchini, S., Tapete, D., Ciampalini, A., Di Traglia, F., Del Ventisette, C., Moretti, S., Casagli, N., 2014b. Multi-temporal evaluation of landslide-induced movements and damage assessment in San Fratello (Italy) by means of C-band and X-band PSI data. In: Pardo-Igúzquiza, E., Guardiola-Albert, C., Heredia, J., Moreno-Merino, L., Durán, J.J., Vargas-Guzmán, J.A. (Eds.), *Mathematics of Planet Earth, Lecture Notes in Earth System Sciences*. Springer, Berlin Heidelberg, pp. 257–261.
- Billi, A., Funicello, R., Minelli, L., Faccenna, C., Neri, G., Orecchio, B., Presti, D., 2008. On the cause of the 1908 Messina tsunami, southern Italy. *Geophys. Res. Lett.* 35, L06301. <http://dx.doi.org/10.1029/2008GL033251>.
- Breiman, L., 2001. Random forests. *Mach. Learn.* 45, 5–32.
- Carbone, S., Catalano, S., Grasso, M., Lentini, F., Monaco, C., 1990. Carta Geologica della Sicilia centro-orientale. Università di Catania, scale 1:50,000.
- Casagli, N., Tibaldi, A., Merri, A., Del Ventisette, C., Apuani, T., Guerri, L., Fortuny-Guasch, J., Tarchi, D., 2009. Deformation of Stromboli Volcano (Italy) during the 2007 eruption revealed by radar interferometry, numerical modelling and structural geological field data. *J. Volcanol. Geotherm. Res.* 182, 182–200.
- Casagli, N., Catani, F., Del Ventisette, C., Luzi, G., 2010. Monitoring, prediction, and early warning using ground-based radar interferometry. *Landslides* 7, 291–301.
- Cascini, L., Fornaro, G., Peduto, D., 2009. Analysis at medium scale of low-resolution DInSAR data in slow-moving landslide-affected areas. *ISPRS J. Photogramm. Remote Sens.* 64, 598–611.
- Cascini, L., Fornaro, G., Peduto, D., 2010. Advanced low- and full-resolution DInSAR map generation for slow-moving landslide analysis at different scales. *Eng. Geol.* 112, 29–42.
- Catani, F., Lagomarsino, D., Segoni, S., Tofani, V., 2013. Exploring model sensitivity issues across different scales in landslide susceptibility. *Nat. Hazards Earth Syst. Sci.* 13, 2815–2831.
- Ciampalini, A., Cigna, F., Del Ventisette, C., Moretti, S., Liguori, V., Casagli, N., 2012. Integrated geomorphological mapping in the north-western sector of Agrigento (Italy). *J. Maps* 8, 136–145.
- Ciampalini, A., Bardi, F., Bianchini, S., Frodella, W., Del Ventisette, C., Moretti, S., Casagli, N., 2014. Analysis of building deformation in landslide area using multisensor PSInSAR™ technique. *Int. J. Appl. Earth Obs. Geoinf.* 33, 166–180.
- Colombo, A., Lanterni, L., Ramasco, M., Troisi, C., 2005. Synthetic GIS-based landslide inventory as the first step for effective landslide-hazard-management. *Landslides* 2, 291–301.
- Corrado, S., Aldega, L., Balestrieri, M.L., Maniscalco, R., Grasso, M., 2009. Structural evolution of the sedimentary accretionary wedge of the alpine system in Eastern Sicily: thermal and thermochronological constraints. *Geol. Soc. Am. Bull.* 121, 1475–1490.
- Crosetto, M., Monserrat, O., Iglesias, R., Crippa, B., 2010. Persistent Scatterer Interferometry: potential, limits and initial C-band and X-band comparison. *Photogramm. Eng. Remote Sens.* 76, 1061–1069.
- Cruden, D.M., Varnes, D.J., 1996. Landslide types and processes. In: Turner, A.K., Shuster, R.L. (Eds.), *Landslides: Investigation and Mitigation*. Spec. Rep 247. Transp. Res. Board, Washington D.C., pp. 36–75.
- De Guidi, G., Lanzafame, G., Palano, M., Puglisi, G., Scaltrito, A., Scarfi, L., 2013. Multidisciplinary study of the Tindari Fault (Sicily, Italy) separating ongoing contractional and extensional compartments along the active Africa–Eurasia convergent boundary. *Tectonophysics* 588, 1–17.
- Del Ventisette, C., Garfagnoli, F., Ciampalini, A., Battistini, A., Gigli, G., Moretti, S., Casagli, N., 2012. An integrated approach to the study of catastrophic debris-flow: geological hazard and human influence. *Nat. Hazards Earth Syst. Sci.* 12, 2907–2922.
- Del Ventisette, C., Ciampalini, A., Manunta, M., Calò, F., Paglia, L., Ardizzone, F., Mondini, A.C., Reichembach, P., Mateos, R.M., Bianchini, S., Garcia, I., Füsü, B., Deak, Z.V., Radi, K., Graniczny, M., Kowalski, Z., Piatkowska, A., Przyłucka, M., Retzo, H., Strozzi, T., Colombo, D., Mora, O., Sanches, F., Herrera, G., Moretti, S., Casagli, S., Guzzetti, F., 2013. Exploitation of large archives of ERS and ENVISAT C-band SAR data to characterize ground deformations. *Remote Sens.* 5, 3896–3917.
- Dellow, G.D., Glassey, P.J., Lukovic, B., Word, P.R., Morrison, B., 2003. Data sources of the New Zealand landslide database. *Geophys. Res. Abstr.* 5, 13867.
- Devoli, G., Strauch, W., Chávez, G., Hoeg, K., 2007. A landslide database for Nicaragua: a tool for landslide-hazard management. *Landslides* 4, 163–176.
- Dewey, J.F., Helman, M.L., Turco, E., Hutton, D.H.W., Knott, S.D., 1989. Kinematics of the western Mediterranean. In: Coward, M.P., Dietrich, D., Parks, R.G. (Eds.), *Alpine tectonics*. Spec. Publ. Geol. Soc. London 45, pp. 265–283.
- Di Paolo, L., Olivetti, V., Corrado, S., Aldega, L., Balestrieri, M.L., Maniscalco, R., 2014. Detecting the stepwise propagation of the Eastern Sicily thrust belt (Italy): insight from thermal and thermochronological constraints. *Terra Nova* 26, 363–371.
- Di Stefano, E., Agate, M., Incarbona, A., Russo, F., Sprovieri, R., Bonomo, S., 2012. Late Quaternary high uplift rates in northeastern Sicily: evidences from calcareous nannofossils and benthic and planktonic foraminifera. *Facies* 58, 1–15.
- Di Traglia, F., Intrieri, E., Nolesini, T., Bardi, F., Del Ventisette, C., Ferrigno, F., Frangioni, S., Frodella, W., Gigli, G., Lotti, A., Tacconi Stefanelli, C., Tanteri, L., Leva, D., Casagli, N., 2014a. The ground-based InSAR monitoring system at Stromboli volcano: linking changes in displacement rate and intensity of persistent volcanic activity. *Bull. Volcanol.* 76, 1–18.
- Di Traglia, F., Cauchie, L., Casagli, N., Saccorotti, G., 2014b. Decrypting geophysical signals at Stromboli Volcano (Italy): integration of seismic and ground-based InSAR displacement data. *Geophys. Res. Lett.* 41, 2753–2761.
- Ferretti, A., Prati, C., Rocca, F., 2000. Non-linear subsidence rate estimation using permanent scatterers in differential SAR interferometry. *IEEE Trans. Geosci. Remote Sens.* 38, 2202–2212.
- Ferretti, A., Prati, C., Rocca, F., 2001. Permanent scatterers in SAR interferometry. *IEEE Trans. Geosci. Remote Sens.* 39, 8–20.
- Ferretti, A., Fumagalli, A., Novati, F., Prati, C., Rocca, F., Rucci, A., 2011. A new algorithm for processing interferometric data-stacks: SqueeSAR. *IEEE Trans. Geosci. Remote Sens.* 49, 3460–3470.
- Gaspar, J.L., Coulart, C., Queiroz, G., Silveira, D., Gomes, A., 2004. Dynamic structure and data sets of a GIS database for geological risk analysis in the Azores volcanic islands. *Nat. Hazards Earth Syst. Sci.* 4, 233–242.
- Gigli, G., Fanti, R., Canuti, P., Casagli, N., 2011. Integration of advanced monitoring and numerical modeling techniques for the complete risk scenario analysis of rockslides: the case of Mt. Beni (Florence, Italy). *Eng. Geol.* 120, 48–59.
- Gustavsson, M., Seijmonsbergen, A.C., Kolstrup, E., 2008. Structure and contents of a new geomorphological GIS database linked to a geomorphological map – With an example from Linden, central Sweden. *Geomorphology* 95, 335–349.
- Guzzetti, F., 2000. Landslide fatalities and evaluation of landslide risk in Italy. *Eng. Geol.* 58, 89–107.
- Guzzetti, F., Cardinali, M., Reichembach, P., 1994. The AVI project: a bibliographical and archive inventory of landslides and floods in Italy. *Environ. Manag.* 18, 623–633.
- Guzzetti, F., Mondini, A.C., Cardinali, M., Fiorucci, F., Santangelo, M., Chang, K.T., 2012. Landslide inventory maps: new tools for an old problem. *Earth Sci. Rev.* 112, 42–66.
- Hanssen, R.F., 2005. Satellite radar interferometry for deformation monitoring: a prior assessment of feasibility and accuracy. *Int. J. Appl. Earth Obs. Geoinf.* 6, 253–260.
- Herrera, G., Gutiérrez, F., García-Davalillo, J.C., Guerrero, J., Notti, D., Galve, J.P., Fernández-Merodo, J.A., Cookley, G., 2013. Multi-sensor advanced DInSAR monitoring of very slow landslides: the Tena Valley case study (Central Spanish Pyrenees). *Remote Sens. Environ.* 128, 31–43.
- Intrieri, E., Di Traglia, F., Del Ventisette, C., Gigli, G., Mugnai, F., Luzi, G., Casagli, N., 2013. Flank instability of Stromboli volcano (Aeolian Islands, Southern Italy): integration of GB-InSAR and geomorphological observations. *Geomorphology* 201, 60–69.
- Klose, M., Damm, B., Terhorst, B., 2014. Landslide cost modeling for transportation infrastructures: a methodological approach. *Landslides* <http://dx.doi.org/10.1007/s10346-014-0481-1>.
- Lagomarsino, D., Segoni, S., Fanti, R., Catani, F., Casagli, N., 2014. Regional scale landslide susceptibility mapping in Emilia Romagna (Italy) as a tool for early warning. *Landslide Science for a Safer Geoenvironment*, pp. 443–449.
- Meisina, C., Notti, D., Zucca, F., Ceriani, M., Colombo, A., Poggi, F., Roccati, A., Zaccone, A., 2013. The use of PSInSAR™ and SqueeSAR™ techniques for updating landslide inventories. In: Margottini, C., Canuti, P., Sassa, K. (Eds.), *Landslide Science and Practice*. Springer, Berlin Heidelberg, pp. 263–266.
- Messina, A., Somma, R., Careri, G., Carbone, G., Macaone, E., 2004. Peloritani continental crust composition (southern Italy): geological and petrochemical evidences. *Boll. Soc. Geol. Ital.* 123, 405–441.
- Nolesini, T., Di Traglia, F., Del Ventisette, C., Moretti, S., Casagli, N., 2013. Deformations and slope instability on Stromboli volcano: integration of GBInSAR data and analog modeling. *Geomorphology* 180, 242–254.
- Notti, D., Davalillo, J.C., Herrera, G., Mora, O., 2010. Assessment of the performance of X-band satellite radar data for landslide mapping and monitoring: Upper Tena Valley case study. *Nat. Hazards Earth Syst. Sci.* 10, 1865–1875.
- Notti, D., Herrera, G., Bianchini, S., Meisina, C., García-Davalillo, J.C., Zucca, F., 2014. A methodology for improving landslide PSI data analysis. *Int. J. Remote Sens.* 35, 2186–2214.
- Pagliara, P., Basile, G., Cara, P., Corazza, A., Duro, A., Manfrè, B., Onori, R., Proietti, C., Sansone, V., 2014. Integration of earth observation and ground-based HR data in the civil protection emergency cycle: the case of the DORIS project. In: Pardo-Igúzquiza, E., Guardiola-Albert, C., Heredia, J., Moreno-Merino, L., Durán, J.J., Vargas-Guzmán, J.A. (Eds.), *Mathematics of Planet Earth, Lecture Notes in Earth System Sciences*. Springer, Berlin Heidelberg, pp. 263–266.
- PAI-Piano Stralcio di Bacino per l'Assetto Idrogeologico, 2012. AdB Regione Sicilia. <http://www.sirh.regione.sicilia.it/pai>.
- Pereira, S., Zêzere, J.L., Quaresma, I.D., Bateira, C., 2014. Landslide incidence in the North of Portugal: analysis of a historical landslide database based on press releases and technical reports. *Geomorphology* 214, 514–525.
- Plank, S., Singer, J., Minet, C., Thuro, K., 2012. Pre-survey suitability evaluation of the differential synthetic aperture radar interferometry method for landslide monitoring. *Int. J. Remote Sens.* 33, 6623–6637.

- Raspini, F., Moretti, S., Casagli, N., 2013. Landslide mapping using SqueeSAR data: Giampilieri (Italy) case study. In: Margottini, C., Canuti, P., Sassa, K. (Eds.), *Landslide Science and Practice*. Springer, Berlin Heidelberg, pp. 147–154.
- Raucoules, D., Bourguin, B., Michele, M., Le Gozannet, G., Closset, L., Bremmer, C., Veldkamp, H., Tragheim, D., Bateson, L., Crosetto, M., Agudo, M., Engdahl, M., 2009. Validation and intercomparison of persistent scatterers interferometry: PSIC4 project results. *J. Appl. Geophys.* 68, 335–347.
- Righini, G., Pancioli, V., Casagli, N., 2012. Updating landslide inventory maps using Persistent Scatterer Interferometry (PSI). *Int. J. Remote Sens.* 33, 2068–2096.
- Suprechi, L., Floris, M., Ghirrotti, M., Genevois, R., Jaboyedoff, M., Stead, D., 2010. Technical note: implementation of a geo-database of published and unpublished data on the catastrophic Vaiont landslide. *Nat. Hazards Earth Syst. Sci.* 10, 865–873.
- Tarchi, D., Casagli, N., Moretti, S., Leva, D., Sieber, A.J., 2003a. Monitoring landslide displacements by using ground-based radar interferometry: application to the Ruinon landslide in the Italian Alps. *J. Geophys. Res.* 108, 101–114.
- Tarchi, D., Casagli, N., Fanti, R., Leva, D., Luzi, G., Pasuto, A., Pieraccini, M., Silvano, S., 2003b. Landslide monitoring by using ground-based SAR interferometry: an example of application to the Tessina landslide in Italy. *Eng. Geol.* 68, 15–30.
- Thomas, M.F.H., Bodin, S., Redfern, J., Irving, D.H.B., 2010. A constrained African craton source for the Cenozoic Numidian Flysch: implications for the palaeogeography of the western Mediterranean basin. *Earth-Sci. Rev.* 101, 1–23.
- Van Den Eeckhaut, M., Hervás, J., 2012. State of the art of national landslide databases in Europe and their potential for assessing landslide susceptibility, hazard and risk. *Geomorphology* 139–140, 545–558.
- van Westen, C.J., Van Asch, T.W.J., Soeters, R., 2005. Landslide hazard and risk zonation: why is it still so difficult? *Bull. Eng. Geol. Environ.* 65, 167–184.
- Werner, C., Wegmüller, U., Strozzi, T., Wiesmann, A., 2003. Interferometric Point Target Analysis for deformation mapping. *Proceedings of IGARSS 2003, Toulouse (France)* 7, pp. 4362–4364.
- Zêzere, J.L., Pereira, S., Tavares, A.O., Bateira, C., Trigo, R.M., Quaresma, I., Santos, P.P., Santos, M., Verde, J., 2014. DISASTER: a GIS database on hydro-geomorphologic disaster in Portugal. *Nat. Hazards* 72, 503–532.